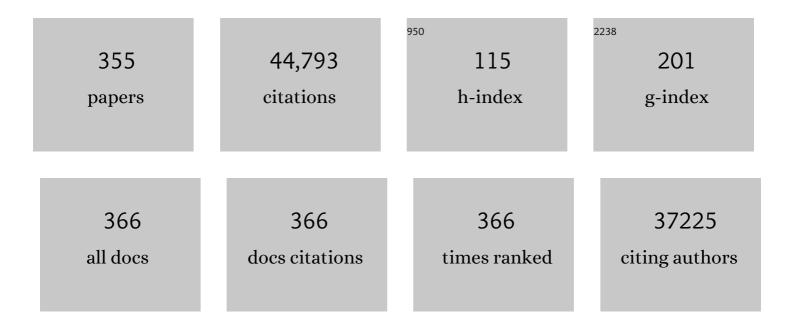
Jimmy C Yu

List of Publications by Year in descending order

Source: https://exaly.com/author-pdf/2340060/publications.pdf Version: 2024-02-01



Іімму С Ун

#	Article	IF	CITATIONS
1	Photocatalytically recovering hydrogen energy from wastewater treatment using MoS2 @TiO2 with sulfur/oxygen dual-defect. Applied Catalysis B: Environmental, 2022, 303, 120878.	10.8	70
2	Panoramic insights into semi-artificial photosynthesis: origin, development, and future perspective. Energy and Environmental Science, 2022, 15, 529-549.	15.6	30
3	Efficient generation of singlet oxygen on modified g-C3N4 photocatalyst for preferential oxidation of targeted organic pollutants. Chemical Engineering Journal, 2022, 431, 134241.	6.6	77
4	Hydrogen Peroxide Production from Water Oxidation on a CuWO ₄ Anode in Oxygen-Deficient Conditions for Water Decontamination. ACS Applied Materials & Interfaces, 2022, 14, 7878-7887.	4.0	14
5	Direct Hydrogen Peroxide Synthesis on a Sn-doped CuWO ₄ /Sn Anode and an Air-Breathing Cathode. Chemistry of Materials, 2022, 34, 63-71.	3.2	6
6	Hetero-phase dendritic elemental phosphorus for visible light photocatalytic hydrogen generation. Applied Catalysis B: Environmental, 2022, 312, 121428.	10.8	15
7	High-performance seawater oxidation by a homogeneous multimetallic layered double hydroxide electrocatalyst. Proceedings of the National Academy of Sciences of the United States of America, 2022, 119, e2202382119.	3.3	51
8	High carbon utilization in CO2 reduction to multi-carbon products in acidic media. Nature Catalysis, 2022, 5, 564-570.	16.1	197
9	Photodriven Disproportionation of Nitrogen and Its Change to Reductive Nitrogen Photofixation. Angewandte Chemie, 2021, 133, 940-949.	1.6	12
10	Hydrothermal and Pyrolytic Conversion of Biomasses into Catalysts for Advanced Oxidation Treatments. Advanced Functional Materials, 2021, 31, 2006505.	7.8	64
11	Photodriven Disproportionation of Nitrogen and Its Change to Reductive Nitrogen Photofixation. Angewandte Chemie - International Edition, 2021, 60, 927-936.	7.2	61
12	Interfacing Iodineâ€Doped Hydrothermally Carbonized Carbon with <i>Escherichia coli</i> through an "Addâ€on―Mode for Enhanced Lightâ€Driven Hydrogen Production. Advanced Energy Materials, 2021, 11, 2100291.	10.2	34
13	Electronic Optimization by Coupling FeCo Nanoclusters and Pt Nanoparticles to Carbon Nanotubes for Efficient Hydrogen Evolution. ACS Sustainable Chemistry and Engineering, 2021, 9, 5895-5901.	3.2	9
14	Photocatalytic degradation of ibuprofen on S-doped BiOBr. Chemosphere, 2021, 278, 130376.	4.2	60
15	Enhanced Mass Transfer of Oxygen through a Gas–Liquid–Solid Interface for Photocatalytic Hydrogen Peroxide Production. Advanced Functional Materials, 2021, 31, 2106120.	7.8	88
16	Converting cellulose waste into a high-efficiency photocatalyst for Cr(VI) reduction via molecular oxygen activation. Applied Catalysis B: Environmental, 2021, 295, 120253.	10.8	39
17	Dressing Plasmons in Nanoparticle-in-Quasi-Cavity Architectures for Trace-Level Surface-Enhanced Raman Spectroscopy Detection. ACS Applied Nano Materials, 2021, 4, 152-158.	2.4	2
18	Highly selective photocatalytic synthesis of ethylene-derived commodity chemicals on BiOBr nanosheets. Materials Today Physics, 2021, 21, 100551.	2.9	2

#	Article	IF	CITATIONS
19	Fabrication of a Photocatalyst with Biomass Waste for H ₂ O ₂ Synthesis. ACS Catalysis, 2021, 11, 14480-14488.	5.5	54
20	Fe Enhanced Visible-Light-Driven Nitrogen Fixation on BiOBr Nanosheets. Chemistry of Materials, 2020, 32, 1488-1494.	3.2	113
21	Visible-light photocatalysis and charge carrier dynamics of elemental crystalline red phosphorus. Journal of Chemical Physics, 2020, 153, 024707.	1.2	13
22	Onâ€Demand Synthesis of H ₂ O ₂ by Water Oxidation for Sustainable Resource Production and Organic Pollutant Degradation. Angewandte Chemie - International Edition, 2020, 59, 20538-20544.	7.2	96
23	Onâ€Demand Synthesis of H ₂ O ₂ by Water Oxidation for Sustainable Resource Production and Organic Pollutant Degradation. Angewandte Chemie, 2020, 132, 20719-20725.	1.6	23
24	Cu(In,Ga)Se2 for selective and efficient photoelectrochemical conversion of CO2 into CO. Journal of Catalysis, 2020, 384, 88-95.	3.1	36
25	Efficient Ammonia Electrosynthesis from Nitrate on Strained Ruthenium Nanoclusters. Journal of the American Chemical Society, 2020, 142, 7036-7046.	6.6	542
26	Efficient Electronic Transport in Partially Disordered Co ₃ O ₄ Nanosheets for Electrocatalytic Oxygen Evolution Reaction. ACS Applied Energy Materials, 2020, 3, 3071-3081.	2.5	27
27	Liquid bismuth initiated growth of phosphorus microbelts with efficient charge polarization for photocatalysis. Applied Catalysis B: Environmental, 2019, 247, 100-106.	10.8	38
28	Soft nanohand grabs a growing nanoparticle. Materials Chemistry Frontiers, 2019, 3, 1555-1564.	3.2	12
29	Biohybrid photoheterotrophic metabolism for significant enhancement of biological nitrogen fixation in pure microbial cultures. Energy and Environmental Science, 2019, 12, 2185-2191.	15.6	61
30	Enhanced CO ₂ reduction and valuable C ₂₊ chemical production by a CdS-photosynthetic hybrid system. Nanoscale, 2019, 11, 9296-9301.	2.8	71
31	Treated rape pollen: a metal-free visible-light-driven photocatalyst from nature for efficient water disinfection. Journal of Materials Chemistry A, 2019, 7, 9335-9344.	5.2	30
32	Photocatalytic Property of Phosphorus. ACS Symposium Series, 2019, , 155-177.	0.5	3
33	Aerosol-spray metal phosphide microspheres with bifunctional electrocatalytic properties for water splitting. Journal of Materials Chemistry A, 2018, 6, 4783-4792.	5.2	53
34	Graphitic carbon nitride nanosheet wrapped mesoporous titanium dioxide for enhanced photoelectrocatalytic water splitting. Catalysis Today, 2018, 315, 103-109.	2.2	53
35	AglnS2/In2S3 heterostructure sensitization of Escherichia coli for sustainable hydrogen production. Nano Energy, 2018, 46, 234-240.	8.2	76
36	Free-standing red phosphorous/silver sponge monolith as an efficient and easily recyclable macroscale photocatalyst for organic pollutant degradation under visible light irradiation. Journal of Colloid and Interface Science, 2018, 518, 130-139.	5.0	30

#	Article	IF	CITATIONS
37	Facile synthesis of carbon- and oxygen-rich graphitic carbon nitride with enhanced visible-light photocatalytic activity. Catalysis Today, 2018, 310, 26-31.	2.2	30
38	A Hollow Porous CdS Photocatalyst. Advanced Materials, 2018, 30, e1804368.	11.1	204
39	Photocatalytic hydrogen evolution and bacterial inactivation utilizing sonochemical-synthesized g-C3N4/red phosphorus hybrid nanosheets as a wide-spectral-responsive photocatalyst: The role of type I band alignment. Applied Catalysis B: Environmental, 2018, 238, 126-135.	10.8	209
40	High-Efficiency "Working-in-Tandem―Nitrogen Photofixation Achieved by Assembling Plasmonic Gold Nanocrystals on Ultrathin Titania Nanosheets. Journal of the American Chemical Society, 2018, 140, 8497-8508.	6.6	382
41	Graphene modified iron sludge derived from homogeneous Fenton process as an efficient heterogeneous Fenton catalyst for degradation of organic pollutants. Microporous and Mesoporous Materials, 2017, 238, 62-68.	2.2	114
42	Gaining Hands-On Experience with Solid-State Photovoltaics through Constructing a Novel n-Si/CuS Solar Cell. Journal of Chemical Education, 2017, 94, 476-479.	1.1	6
43	Converting Carbohydrates to Carbon-Based Photocatalysts for Environmental Treatment. Environmental Science & Technology, 2017, 51, 7076-7083.	4.6	107
44	Enhanced photocatalytic hydrogen production from aqueous sulfide/sulfite solution by ZnO 0.6 S 0.4 with simultaneous dye degradation under visible-light irradiation. Chemosphere, 2017, 183, 219-228.	4.2	40
45	Earth-abundant Ni2P/g-C3N4 lamellar nanohydrids for enhanced photocatalytic hydrogen evolution and bacterial inactivation under visible light irradiation. Applied Catalysis B: Environmental, 2017, 217, 570-580.	10.8	311
46	A metal-free composite photocatalyst of graphene quantum dots deposited on red phosphorus. Journal of Environmental Sciences, 2017, 60, 91-97.	3.2	24
47	Phosphorus containing materials for photocatalytic hydrogen evolution. Green Chemistry, 2017, 19, 588-613.	4.6	148
48	Effective Prevention of Charge Trapping in Graphitic Carbon Nitride with Nanosized Red Phosphorus Modification for Superior Photo(electro)catalysis. Advanced Functional Materials, 2017, 27, 1703484.	7.8	188
49	Photocatalysis: Effective Prevention of Charge Trapping in Graphitic Carbon Nitride with Nanosized Red Phosphorus Modification for Superior Photo(electro)catalysis (Adv. Funct. Mater. 46/2017). Advanced Functional Materials, 2017, 27, .	7.8	1
50	Intrinsic defect based homojunction: A novel quantum dots photoanode with enhanced charge transfer kinetics. Applied Catalysis B: Environmental, 2017, 203, 829-838.	10.8	30
51	Innenrücktitelbild: An Elemental Phosphorus Photocatalyst with a Record High Hydrogen Evolution Efficiency (Angew. Chem. 33/2016). Angewandte Chemie, 2016, 128, 9947-9947.	1.6	2
52	An Elemental Phosphorus Photocatalyst with a Record High Hydrogen Evolution Efficiency. Angewandte Chemie - International Edition, 2016, 55, 9580-9585.	7.2	171
53	Enhancing Charge Separation in Metallic Photocatalysts: A Case Study of the Conducting Molybdenum Dioxide. Advanced Functional Materials, 2016, 26, 4445-4455.	7.8	154
54	Nanostructured Elemental Photocatalysts: Development and Challenges. Nanostructure Science and Technology, 2016, , 295-312.	0.1	2

#	Article	IF	CITATIONS
55	Redox-responsive controlled DNA transfection and gene silencing based on polymer-conjugated magnetic nanoparticles. RSC Advances, 2016, 6, 72155-72164.	1.7	14
56	Room temperature synthesis of a highly active Cu/Cu ₂ 0 photocathode for photocelectrochemical water splitting. Journal of Materials Chemistry A, 2016, 4, 13736-13741.	5.2	43
57	Enhanced Activity and Stability of Carbon-Decorated Cuprous Oxide Mesoporous Nanorods for CO ₂ Reduction in Artificial Photosynthesis. ACS Catalysis, 2016, 6, 6444-6454.	5.5	201
58	Metallic Photocatalysts: Enhancing Charge Separation in Metallic Photocatalysts: A Case Study of the Conducting Molybdenum Dioxide (Adv. Funct. Mater. 25/2016). Advanced Functional Materials, 2016, 26, 4444-4444.	7.8	1
59	An Elemental Phosphorus Photocatalyst with a Record High Hydrogen Evolution Efficiency. Angewandte Chemie, 2016, 128, 9732-9737.	1.6	41
60	Progress in sonochemical fabrication of nanostructured photocatalysts. Rare Metals, 2016, 35, 211-222.	3.6	25
61	Covalent Fixation of Surface Oxygen Atoms on Hematite Photoanode for Enhanced Water Oxidation. Chemistry of Materials, 2016, 28, 564-572.	3.2	118
62	A NIR-driven photocatalyst based on α-NaYF 4 :Yb,Tm@TiO 2 core–shell structure supported on reduced graphene oxide. Applied Catalysis B: Environmental, 2016, 182, 184-192.	10.8	126
63	A nanostructured chromium(iii) oxide/tungsten(vi) oxide p–n junction photoanode toward enhanced efficiency for water oxidation. Journal of Materials Chemistry A, 2015, 3, 14046-14053.	5.2	57
64	Synthesis of 3D structured graphene as a high performance catalyst support for methanol electro-oxidation. Nanoscale, 2015, 7, 10896-10902.	2.8	25
65	Enhanced photo-Fenton degradation of rhodamine B using graphene oxide–amorphous FePO4 as effective and stable heterogeneous catalyst. Journal of Colloid and Interface Science, 2015, 448, 460-466.	5.0	113
66	Mesoporous carbon/CuS nanocomposites for pH-dependent drug delivery and near-infrared chemo-photothermal therapy. RSC Advances, 2015, 5, 93226-93233.	1.7	42
67	A black–red phosphorus heterostructure for efficient visible-light-driven photocatalysis. Journal of Materials Chemistry A, 2015, 3, 3285-3288.	5.2	232
68	A wide-spectrum-responsive TiO 2 photoanode for photoelectrochemical cells. Applied Catalysis B: Environmental, 2015, 168-169, 483-489.	10.8	27
69	An NIR-triggered and thermally responsive drug delivery platform through DNA/copper sulfide gates. Nanoscale, 2015, 7, 12614-12624.	2.8	49
70	Advances in photocatalytic disinfection of bacteria: Development of photocatalysts and mechanisms. Journal of Environmental Sciences, 2015, 34, 232-247.	3.2	251
71	Red Phosphorus: An Earth-Abundant Elemental Photocatalyst for "Green―Bacterial Inactivation under Visible Light. Environmental Science & Technology, 2015, 49, 6264-6273.	4.6	226
72	Monoclinic dibismuth tetraoxide: A new visible-light-driven photocatalyst for environmental remediation. Applied Catalysis B: Environmental, 2015, 176-177, 444-453.	10.8	153

#	Article	IF	CITATIONS
73	Pt/Bi2WO6 composite microflowers: High visible light photocatalytic performance and easy recycle. Separation and Purification Technology, 2015, 154, 115-122.	3.9	49
74	A visible-light-driven composite photocatalyst of TiO ₂ nanotube arrays and graphene quantum dots. Beilstein Journal of Nanotechnology, 2014, 5, 689-695.	1.5	31
75	Design and fabrication of heterojunction photocatalysts for energy conversion and pollutant degradation. Chinese Journal of Catalysis, 2014, 35, 1609-1618.	6.9	80
76	Assembly of polyethylenimine-functionalized iron oxide nanoparticles as agents for DNA transfection with magnetofection technique. Journal of Materials Chemistry B, 2014, 2, 7936-7944.	2.9	29
77	Microwave hydrothermal synthesis of MSnO3 (M2+Â=ÂCa2+, Sr2+, Ba2+): effect of M2+ on crystal structure and photocatalytic properties. Journal of Materials Science, 2014, 49, 1893-1902.	1.7	33
78	Biomolecule-assisted fabrication of copper doped SnS ₂ nanosheet–reduced graphene oxide junctions with enhanced visible-light photocatalytic activity. Journal of Materials Chemistry A, 2014, 2, 1000-1005.	5.2	144
79	Ultrasonic aerosol spray-assisted preparation of TiO2/In2O3 composite for visible-light-driven photocatalysis. Journal of Catalysis, 2014, 310, 84-90.	3.1	43
80	Direct observation of carbon nanostructure growth at liquid–solid interfaces. Chemical Communications, 2014, 50, 826-828.	2.2	25
81	Crystalline phosphorus fibers: controllable synthesis and visible-light-driven photocatalytic activity. Nanoscale, 2014, 6, 14163-14167.	2.8	91
82	An efficient dye-sensitized BiOCl photocatalyst for air and water purification under visible light irradiation. Environmental Sciences: Processes and Impacts, 2014, 16, 1975-1980.	1.7	66
83	Chemical modification of inorganic nanostructures for targeted and controlled drug delivery in cancer treatment. Journal of Materials Chemistry B, 2014, 2, 452-470.	2.9	108
84	Azobenzene dendronized carbon nanoparticles: the effect of light antenna. RSC Advances, 2014, 4, 18193-18197.	1.7	6
85	Potassium ion-mediated synthesis of highly water-soluble dendritically functionalized melanins. New Journal of Chemistry, 2014, 38, 3362.	1.4	1
86	Selective deposition of redox co-catalyst(s) to improve the photocatalytic activity of single-domain ferroelectric PbTiO ₃ nanoplates. Chemical Communications, 2014, 50, 10416.	2.2	100
87	(Gold Core)@(Ceria Shell) Nanostructures for Plasmon-Enhanced Catalytic Reactions under Visible Light. ACS Nano, 2014, 8, 8152-8162.	7.3	230
88	Switching the selectivity of the photoreduction reaction of carbon dioxide by controlling the band structure of a g-C ₃ N ₄ photocatalyst. Chemical Communications, 2014, 50, 10837.	2.2	192
89	g-C ₃ N ₄ quantum dots: direct synthesis, upconversion properties and photocatalytic application. Chemical Communications, 2014, 50, 10148-10150.	2.2	351
90	Porous TiO ₂ Materials through Pickering High-Internal Phase Emulsion Templating. Langmuir, 2014, 30, 2676-2683.	1.6	67

#	Article	IF	CITATIONS
91	A nonstoichiometric SnO2â [~] î [~] nanocrystal-based counter electrode for remarkably improving the performance of dye-sensitized solar cells. Chemical Communications, 2014, 50, 7020.	2.2	41
92	Fabrication, characterization of \hat{l}^2 -MnO2 microrod catalysts and their performance in rapid degradation of dyes of high concentration. Catalysis Today, 2014, 224, 154-162.	2.2	97
93	Vertically aligned CdTe nanotube arrays on indium tin oxide for visible-light-driven photoelectrocatalysis. Applied Catalysis B: Environmental, 2014, 147, 17-21.	10.8	20
94	Lanthanide stannate pyrochlores Ln2Sn2O7 (Ln=Nd, Sm, Eu, Gd, Er, Yb) nanocrystals: Synthesis, characterization, and photocatalytic properties. Materials Research Bulletin, 2014, 56, 86-91.	2.7	35
95	Removal of nitric oxide by the highly reactive anatase TiO2 (001) surface: A density functional theory study. Journal of Colloid and Interface Science, 2014, 430, 18-23.	5.0	24
96	Preparation, characterization, and photocatalytic properties of Pt/BiOCl nanoplates. Chinese Journal of Catalysis, 2014, 34, 385-390.	6.9	1
97	Graphene and g-C ₃ N ₄ Nanosheets Cowrapped Elemental α-Sulfur As a Novel Metal-Free Heterojunction Photocatalyst for Bacterial Inactivation under Visible-Light. Environmental Science & Technology, 2013, 47, 8724-8732.	4.6	383
98	Novel hollow Pt-ZnO nanocomposite microspheres with hierarchical structure and enhanced photocatalytic activity and stability. Nanoscale, 2013, 5, 2142.	2.8	313
99	Hydrothermal synthesis and characterization of novel PbWO4 microspheres with hierarchical nanostructures and enhanced photocatalytic performance in dye degradation. Chemical Engineering Journal, 2013, 219, 86-95.	6.6	68
100	Novel noble metal (Rh, Pd, Pt)/BiOX(Cl, Br, I) composite photocatalysts with enhanced photocatalytic performance in dye degradation. Separation and Purification Technology, 2013, 120, 110-122.	3.9	152
101	Pt3Co-loaded CdS and TiO2 for photocatalytic hydrogen evolution from water. Journal of Materials Chemistry A, 2013, 1, 12221.	5.2	73
102	Synthesis of porous Bi4Ti3O12 nanofibers by electrospinning and their enhanced visible-light-driven photocatalytic properties. Nanoscale, 2013, 5, 2028.	2.8	143
103	CdIn2S4 microsphere as an efficient visible-light-driven photocatalyst for bacterial inactivation: Synthesis, characterizations and photocatalytic inactivation mechanisms. Applied Catalysis B: Environmental, 2013, 129, 482-490.	10.8	170
104	Ultrasonic fabrication of N-doped TiO2 nanocrystals with mesoporous structure and enhanced visible light photocatalytic activity. Chinese Journal of Catalysis, 2013, 34, 1250-1255.	6.9	46
105	Preparation, characterization and photocatalytic performance of noble metals (Ag, Pd, Pt, Rh) deposited on sponge-like ZnO microcuboids. Journal of Physics and Chemistry of Solids, 2013, 74, 1714-1720.	1.9	55
106	Metal Nanocrystalâ€Embedded Hollow Mesoporous TiO ₂ and ZrO ₂ Microspheres Prepared with Polystyrene Nanospheres as Carriers and Templates. Advanced Functional Materials, 2013, 23, 2137-2144.	7.8	112
107	Synthesis and characterization of Ag/TiO2-B nanosquares with high photocatalytic activity under visible light irradiation. Materials Science and Engineering B: Solid-State Materials for Advanced Technology, 2013, 178, 344-348.	1.7	45
108	Loading Metal Nanostructures on Cotton Fabrics as Recyclable Catalysts. Small, 2013, 9, 1003-1007.	5.2	29

#	Article	IF	CITATIONS
109	Plasmonic Harvesting of Light Energy for Suzuki Coupling Reactions. Journal of the American Chemical Society, 2013, 135, 5588-5601.	6.6	597
110	Plasmon-enhanced chemical reactions. Journal of Materials Chemistry A, 2013, 1, 5790.	5.2	257
111	Graphene oxide–Fe2O3 hybrid material as highly efficient heterogeneous catalyst for degradation of organic contaminants. Carbon, 2013, 60, 437-444.	5.4	335
112	Folate-conjugated Fe3O4@SiO2@gold nanorods@mesoporous SiO2 hybrid nanomaterial: a theranostic agent for magnetic resonance imaging and photothermal therapy. Journal of Materials Chemistry B, 2013, 1, 2934.	2.9	72
113	CdS nanorods/reduced graphene oxide nanocomposites for photocatalysis and electrochemical sensing. Journal of Materials Chemistry A, 2013, 1, 5158.	5.2	101
114	Ultrasound, pH, and Magnetically Responsive Crown-Ether-Coated Core/Shell Nanoparticles as Drug Encapsulation and Release Systems. ACS Applied Materials & Interfaces, 2013, 5, 1566-1574.	4.0	122
115	Enhanced photocatalytic water disinfection properties of Bi2MoO6–RGO nanocomposites under visible light irradiation. Nanoscale, 2013, 5, 6307.	2.8	121
116	One-pot synthesis of In2S3 nanosheets/graphene composites with enhanced visible-light photocatalytic activity. Applied Catalysis B: Environmental, 2013, 129, 80-88.	10.8	145
117	In situ synthesis of Zn2GeO4 hollow spheres and their enhanced photocatalytic activity for the degradation of antibiotic metronidazole. Dalton Transactions, 2013, 42, 5092.	1.6	57
118	Preparation, Characterization and Photocatalytic Performance of Ag/BiOX (X=Cl, Br, I) Composite Photocatalysts. Wuli Huaxue Xuebao/ Acta Physico - Chimica Sinica, 2012, 28, 647-653.	2.2	18
119	Visible-Light-Driven Photocatalytic Inactivation of <i>E. coli</i> K-12 by Bismuth Vanadate Nanotubes: Bactericidal Performance and Mechanism. Environmental Science & Technology, 2012, 46, 4599-4606.	4.6	254
120	Synthesize of Cu2O-CuO/Sr3BiO5.4 and its photocatalytic activity. Applied Surface Science, 2012, 258, 5955-5959.	3.1	9
121	Sonochemical fabrication of novel square-shaped F doped TiO2 nanocrystals with enhanced performance in photocatalytic degradation of phenol. Journal of Hazardous Materials, 2012, 237-238, 38-45.	6.5	83
122	Preparation, characterization and photocatalytic performance of Mo-doped ZnO photocatalysts. Science China Chemistry, 2012, 55, 1802-1810.	4.2	71
123	Facet effect of copper(I) sulfide nanocrystals on photoelectrochemical properties. Progress in Natural Science: Materials International, 2012, 22, 585-591.	1.8	26
124	Photocytotoxicity and Magnetic Relaxivity Responses of Dual-Porous γ-Fe ₂ 0 ₃ @ <i>meso</i> -SiO ₂ Microspheres. ACS Applied Materials & Interfaces, 2012, 4, 2033-2040.	4.0	51
125	WO3 nanorods/graphene nanocomposites for high-efficiency visible-light-driven photocatalysis and NO2 gas sensing. Journal of Materials Chemistry, 2012, 22, 8525.	6.7	484
126	Porous Singleâ€Crystalline Palladium Nanoparticles with High Catalytic Activities. Angewandte Chemie - International Edition, 2012, 51, 4872-4876.	7.2	206

#	Article	IF	CITATIONS
127	Red phosphorus: An elemental photocatalyst for hydrogen formation from water. Applied Catalysis B: Environmental, 2012, 111-112, 409-414.	10.8	265
128	Hierarchical P/YPO4 microsphere for photocatalytic hydrogen production from water under visible light irradiation. Applied Catalysis B: Environmental, 2012, 119-120, 267-272.	10.8	79
129	Ultra-fast method to synthesize mesoporous magnetite nanoclusters as highly sensitive magnetic resonance probe. Journal of Colloid and Interface Science, 2012, 379, 1-7.	5.0	21
130	WO3/TiO2 microstructures for enhanced photocatalytic oxidation. Separation and Purification Technology, 2012, 91, 67-72.	3.9	26
131	Hexagonal tungsten trioxide nanorods as a rapid adsorbent for methylene blue. Separation and Purification Technology, 2012, 91, 103-107.	3.9	32
132	Ionothermal synthesis of hierarchical BiOBr microspheres for water treatment. Journal of Hazardous Materials, 2012, 211-212, 104-111.	6.5	126
133	Hierarchical core/shell Fe3O4@SiO2@ ^{ĵ3} -AlOOH@Au micro/nanoflowers for protein immobilization. Chemical Communications, 2011, 47, 2514.	2.2	56
134	Advanced Photocatalytic Nanomaterials for Degrading Pollutants and Generating Fuels by Sunlight. Green Energy and Technology, 2011, , 679-716.	0.4	6
135	Nanoflower arrays of rutile TiO2. Chemical Communications, 2011, 47, 1184-1186.	2.2	50
136	Morphosynthesis of a hierarchical MoO2 nanoarchitecture as a binder-free anode for lithium-ion batteries. Energy and Environmental Science, 2011, 4, 2870.	15.6	245
137	Synthesis of Biocompatible, Mesoporous Fe ₃ O ₄ Nano/Microspheres with Large Surface Area for Magnetic Resonance Imaging and Therapeutic Applications. ACS Applied Materials & Interfaces, 2011, 3, 237-244.	4.0	197
138	Porous upconversion materials-assisted near infrared energy harvesting by chlorophylls. Chemical Communications, 2011, 47, 3511.	2.2	8
139	Heteroepitaxial Growth of High-Index-Faceted Palladium Nanoshells and Their Catalytic Performance. Journal of the American Chemical Society, 2011, 133, 1106-1111.	6.6	287
140	Effects of Cu2O nanoparticle and CuCl2 on zebrafish larvae and a liver cell-line. Aquatic Toxicology, 2011, 105, 344-354.	1.9	75
141	Graphene-based photocatalytic composites. RSC Advances, 2011, 1, 1426.	1.7	499
142	Fast fabrication of Co3O4 and CuO/BiVO4 composite photocatalysts with high crystallinity and enhanced photocatalytic activity via ultrasound irradiation. Journal of Alloys and Compounds, 2011, 509, 4547-4552.	2.8	100
143	Crystal facet engineering of semiconductor photocatalysts: motivations, advances and unique properties. Chemical Communications, 2011, 47, 6763.	2.2	867
144	Preparation of bismuth oxyiodides and oxides and their photooxidation characteristic under visible/UV light irradiation. Materials Research Bulletin, 2011, 46, 140-146.	2.7	79

#	Article	IF	CITATIONS
145	Semiconductor/biomolecular composites for solar energy applications. Energy and Environmental Science, 2011, 4, 100-113.	15.6	75
146	Preparation of WO3/ZnO Composite Photocatalyst and Its Photocatalytic Performance. Chinese Journal of Catalysis, 2011, 32, 555-565.	6.9	114
147	Hydrothermal Synthesis and Photocatalytic Performance of Bi ₂ WO ₆ /ZnO Heterojunction Photocatalysts. Wuji Cailiao Xuebao/Journal of Inorganic Materials, 2011, 26, 1157-1163.	0.6	15
148	Facile synthesis of size-controllable monodispersed ferrite nanospheres. Journal of Materials Chemistry, 2010, 20, 5086.	6.7	197
149	WO3 Coupled P-TiO2 Photocatalysts with Mesoporous Structure. Catalysis Letters, 2010, 140, 172-183.	1.4	67
150	On the Origin of the Visibleâ€Light Activity of Titanium Dioxide Doped with Carbonate Species. ChemPhysChem, 2010, 11, 3269-3272.	1.0	10
151	Induced Crystallization of Rubrene in Thinâ€Film Transistors. Advanced Materials, 2010, 22, 3242-3246.	11.1	67
152	Induced Crystallization of Rubrene in Thinâ€Film Transistors (Adv. Mater. 30/2010). Advanced Materials, 2010, 22, .	11.1	4
153	Sol–gel derived S,I-codoped mesoporous TiO2 photocatalyst with high visible-light photocatalytic activity. Journal of Physics and Chemistry of Solids, 2010, 71, 1337-1343.	1.9	70
154	Synthesis and characterization of Pt/BiOI nanoplate catalyst with enhanced activity under visible light irradiation. Materials Science and Engineering B: Solid-State Materials for Advanced Technology, 2010, 166, 213-219.	1.7	161
155	NaYF4:Yb,Tm/CdS composite as a novel near-infrared-driven photocatalyst. Applied Catalysis B: Environmental, 2010, 100, 433-439.	10.8	165
156	Monosteps on the Surfaces of Mesostructured Silica and Titania Thin Films. Small, 2010, 6, 1880-1885.	5.2	6
157	Green synthesis of a self-assembled rutile mesocrystalline photocatalyst. CrystEngComm, 2010, 12, 1759.	1.3	84
158	Design, Fabrication, and Modification of Nanostructured Semiconductor Materials for Environmental and Energy Applications. Langmuir, 2010, 26, 3031-3039.	1.6	464
159	Biocompatible Anatase Single-Crystal Photocatalysts with Tunable Percentage of Reactive Facets. Crystal Growth and Design, 2010, 10, 1130-1137.	1.4	120
160	Effective Photocatalytic Disinfection of <i>E. coli</i> K-12 Using AgBrâ^'Agâ^'Bi ₂ WO ₆ Nanojunction System Irradiated by Visible Light: The Role of Diffusing Hydroxyl Radicals. Environmental Science & Technology, 2010, 44, 1392-1398.	4.6	557
161	An Efficient Bismuth Tungstate Visible-Light-Driven Photocatalyst for Breaking Down Nitric Oxide. Environmental Science & Technology, 2010, 44, 4276-4281.	4.6	170
162	Magnetic Nanochains of FeNi ₃ Prepared by a Template-Free Microwave-Hydrothermal Method. ACS Applied Materials & Interfaces, 2010, 2, 2579-2584.	4.0	59

#	Article	IF	CITATIONS
163	Inorganic materials for photocatalytic water disinfection. Journal of Materials Chemistry, 2010, 20, 4529.	6.7	173
164	Photochemical growth of nanoporous SnO2 at the air–water interface and its high photocatalytic activity. Journal of Materials Chemistry, 2010, 20, 5641.	6.7	133
165	Growth of single-crystalline SnO ₂ nanocubes via a hydrothermal route. CrystEngComm, 2010, 12, 341-343.	1.3	28
166	A mild solvothermal route for preparation of cubic-like CuInS2 crystals. Materials Letters, 2009, 63, 1984-1986.	1.3	34
167	Sonochemical fabrication of fluorinated mesoporous titanium dioxide microspheres. Journal of Solid State Chemistry, 2009, 182, 1061-1069.	1.4	105
168	A Simple Way to Prepare C–N-Codoped TiO2 Photocatalyst with Visible-Light Activity. Catalysis Letters, 2009, 129, 462-470.	1.4	139
169	Sonochemical fabrication, characterization and photocatalytic properties of Ag/ZnWO4 nanorod catalyst. Materials Science and Engineering B: Solid-State Materials for Advanced Technology, 2009, 164, 16-22.	1.7	103
170	Simultaneous photocatalytic removal of ammonium and nitrite in water using Ce3+–Ag+ modified TiO2. Separation and Purification Technology, 2009, 67, 244-248.	3.9	13
171	A mesoporous TiO2â^'xNx photocatalyst prepared by sonication pretreatment and in situ pyrolysis. Separation and Purification Technology, 2009, 67, 152-157.	3.9	24
172	AgBr-Ag-Bi2WO6 nanojunction system: A novel and efficient photocatalyst with double visible-light active components. Applied Catalysis A: General, 2009, 363, 221-229.	2.2	304
173	Preparation, Characterization, and Catalytic Activity of Core/Shell Fe ₃ O ₄ @Polyaniline@Au Nanocomposites. Langmuir, 2009, 25, 11835-11843.	1.6	351
174	Cross-Medal Arrays of Ta-Doped Rutile Titania. Journal of the American Chemical Society, 2009, 131, 12048-12049.	6.6	35
175	Zn:ln(OH) _{<i>y</i>} S _{<i>z</i>} Solid Solution Nanoplates: Synthesis, Characterization, and Photocatalytic Mechanism. Environmental Science & Technology, 2009, 43, 7883-7888.	4.6	76
176	Degradation of Acid Orange 7 using magnetic AgBr under visible light: The roles of oxidizing species. Chemosphere, 2009, 76, 1185-1191.	4.2	386
177	Synthesis of Size-Tunable Monodispersed Metallic Nickel Nanocrystals without Hot Injection. Crystal Growth and Design, 2009, 9, 2812-2815.	1.4	31
178	Tuning the Grain Size and Particle Size of Superparamagnetic Fe ₃ O ₄ Microparticles. Chemistry of Materials, 2009, 21, 5079-5087.	3.2	387
179	A New Visible-Light Photocatalyst: CdS Quantum Dots Embedded Mesoporous TiO ₂ . Environmental Science & Technology, 2009, 43, 7079-7085.	4.6	413
180	Discrete Functional Gold Nanoparticles: Hydrogen Bond-Assisted Synthesis, Magnetic Purification, Supramolecular Dimer and Trimer Formation. ACS Nano, 2009, 3, 2129-2138.	7.3	56

#	Article	IF	CITATIONS
181	Photochemical growth of cadmium-rich CdS nanotubes at the air–water interface and their use in photocatalysis. Journal of Materials Chemistry, 2009, 19, 6901.	6.7	48
182	A micrometer-size TiO2 single-crystal photocatalyst with remarkable 80% level of reactive facets. Chemical Communications, 2009, , 4381.	2.2	327
183	Thermally stable ordered mesoporous CeO2/TiO2 visible-light photocatalysts. Physical Chemistry Chemical Physics, 2009, 11, 3775.	1.3	152
184	Hierarchically Nanostructured Rutile Arrays: Acid Vapor Oxidation Growth and Tunable Morphologies. ACS Nano, 2009, 3, 1212-1218.	7.3	105
185	A Meaningful Analogue of Pentacene: Charge Transport, Polymorphs, and Electronic Structures of Dihydrodiazapentacene. Chemistry of Materials, 2009, 21, 1400-1405.	3.2	63
186	Direct encoding of silica submicrospheres with cadmium telluride nanocrystals. Journal of Materials Chemistry, 2009, 19, 7002.	6.7	20
187	Porous Sr2CuWO6 Nanoarchitectures Fabricated by a Matrix-mediated Route. Chemistry Letters, 2009, 38, 320-321.	0.7	0
188	A lamellar ceria structure with encapsulated platinum nanoparticles. Nano Research, 2008, 1, 474-482.	5.8	8
189	Continuous Aspectâ€Ratio Tuning and Fine Shape Control of Monodisperse <i>α</i> â€Fe ₂ O ₃ Nanocrystals by a Programmed Microwave–Hydrothermal Method. Advanced Functional Materials, 2008, 18, 880-887.	7.8	246
190	Continuous Size Tuning of Monodisperse ZnO Colloidal Nanocrystal Clusters by a Microwaveâ€Polyol Process and Their Application for Humidity Sensing. Advanced Materials, 2008, 20, 4845-4850.	11.1	242
191	Fibrous TiO2 prepared by chemical vapor deposition using activated carbon fibers as template via adsorption, hydrolysis and calcinations. Journal of Zhejiang University: Science A, 2008, 9, 981-987.	1.3	4
192	High-Yield Synthesis of Nickel and Nickel Phosphide Nanowires via Microwave-Assisted Processes. Chemistry of Materials, 2008, 20, 6743-6749.	3.2	93
193	Ordered Mesoporous BiVO ₄ through Nanocasting: A Superior Visible Light-Driven Photocatalyst. Chemistry of Materials, 2008, 20, 3983-3992.	3.2	340
194	Effect of Carbon Doping on the Mesoporous Structure of Nanocrystalline Titanium Dioxide and Its Solar-Light-Driven Photocatalytic Degradation of NO <i>_x</i> . Langmuir, 2008, 24, 3510-3516.	1.6	288
195	Photocatalytic disinfection of marine bacteria using fluorescent light. Water Research, 2008, 42, 4827-4837.	5.3	100
196	A Novel Intermediate-Sacrificed Route to Polycrystalline Nanorods Consisting of Highly Oriented Quantum Dots of Cubic CdS. Journal of Nanoscience and Nanotechnology, 2008, 8, 3112-3116.	0.9	2
197	Fe3+/Fe2+ cycling promoted by Ta3N5 under visible irradiation in Fenton degradation of organic pollutants. Applied Catalysis B: Environmental, 2007, 75, 256-263.	10.8	40
198	A Facile Surface-Etching Route to Thin Films of Metal Iodides. Crystal Growth and Design, 2007, 7, 262-267.	1.4	20

#	Article	IF	CITATIONS
199	Facile Decoring Route to Carbon Nano Test Tubes. Journal of Physical Chemistry C, 2007, 111, 5830-5834.	1.5	14
200	Fast Production of Self-Assembled Hierarchical α-Fe ₂ O ₃ Nanoarchitectures. Journal of Physical Chemistry C, 2007, 111, 11180-11185.	1.5	140
201	Rapid Mass Production of Hierarchically Porous ZnIn2S4Submicrospheres via a Microwave-Solvothermal Process. Crystal Growth and Design, 2007, 7, 2444-2448.	1.4	122
202	Photochemical Preparation of Two-Dimensional Gold Spherical Pore and Hollow Sphere Arrays on a Solution Surface. Angewandte Chemie - International Edition, 2007, 46, 773-777.	7.2	57
203	αâ€Fe ₂ O ₃ Nanorings Prepared by a Microwaveâ€Assisted Hydrothermal Process and Their Sensing Properties. Advanced Materials, 2007, 19, 2324-2329.	11.1	602
204	Hierarchical mesoporous grape-like titania with superior recyclability and photoactivity. Microporous and Mesoporous Materials, 2007, 106, 278-283.	2.2	24
205	Photocatalytic activity and photo-induced hydrophilicity of mesoporous TiO2 thin films coated on aluminum substrate. Applied Catalysis B: Environmental, 2007, 73, 135-143.	10.8	40
206	Large-scale in situ synthesis and characterization of ternary single-crystal NaV6O15 nanoneedles. Materials Chemistry and Physics, 2007, 104, 362-366.	2.0	16
207	Preparation and biomedical application of a non-polymer coated superparamagnetic nanoparticle. International Journal of Nanomedicine, 2007, 2, 805-12.	3.3	8
208	Synthesis and Characterization of TiO2@C Coreâ^'Shell Composite Nanoparticles and Evaluation of Their Photocatalytic Activities. Chemistry of Materials, 2006, 18, 2275-2282.	3.2	166
209	Synthesis of surface-functionalized t-Se microspheres via a green wet-chemical route. Journal of Materials Chemistry, 2006, 16, 748-751.	6.7	19
210	ZrO2-Modified Mesoporous Nanocrystalline TiO2-xNxas Efficient Visible Light Photocatalysts. Environmental Science & Technology, 2006, 40, 2369-2374.	4.6	224
211	An ordered cubic Im3m mesoporous Cr–TiO2visible light photocatalyst. Chemical Communications, 2006, , 2717-2719.	2.2	117
212	Comparison of Photocatalytic Oxidation and Ozonation in Degrading of Polycyclic Aromatic Hydrocarbons. Human and Ecological Risk Assessment (HERA), 2006, 12, 270-276.	1.7	7
213	Construction of Size-Controllable Hierarchical Nanoporous TiO2Ring Arrays and Their Modifications. Chemistry of Materials, 2006, 18, 3774-3779.	3.2	68
214	Photocatalytic oxidation of triclosan. Chemosphere, 2006, 65, 390-399.	4.2	106
215	Sonochemical synthesis and visible light photocatalytic behavior of CdSe and CdSe/TiO2 nanoparticles. Journal of Molecular Catalysis A, 2006, 247, 268-274.	4.8	146
216	Probing of photocatalytic surface sites on SO42â^'/TiO2 solid acids by in situ FT-IR spectroscopy and pyridine adsorption. Journal of Photochemistry and Photobiology A: Chemistry, 2006, 179, 339-347.	2.0	184

#	Article	IF	CITATIONS
217	Characterization and photocatalytic mechanism of nanosized CdS coupled TiO2 nanocrystals under visible light irradiation. Journal of Molecular Catalysis A, 2006, 244, 25-32.	4.8	415
218	Preparation, characterization and photocatalytic activity of in situ Fe-doped TiO2 thin films. Thin Solid Films, 2006, 496, 273-280.	0.8	154
219	Synthesis of hierarchical nanoporous F-doped TiO2 spheres with visible light photocatalytic activity. Chemical Communications, 2006, , 1115.	2.2	359
220	Microwave-Assisted Synthesis of a Superparamagnetic Surface-Functionalized Porous Fe3O4/C Nanocomposite. Chemistry - an Asian Journal, 2006, 1, 605-610.	1.7	36
221	Low-temperature hydrothermal synthesis of S-doped TiO2 with visible light photocatalytic activity. Journal of Solid State Chemistry, 2006, 179, 1171-1176.	1.4	245
222	Preparation and characterization of nanoplatelets of nickel hydroxide and nickel oxide. Materials Chemistry and Physics, 2006, 98, 267-272.	2.0	29
223	Synthesis and Characterization of Core-Shell Selenium/Carbon Colloids and Hollow Carbon Capsules. Chemistry - A European Journal, 2006, 12, 548-552.	1.7	66
224	Controlled Hydrothermal Synthesis and Growth Mechanism of Various Nanostructured Films of Copper and Silver Tellurides. Chemistry - A European Journal, 2006, 12, 4185-4190.	1.7	55
225	Determination of Total Gaseous Lead in the Atmosphere by Honeycomb Denuder/Electrothermal Atomic Absorption Spectrometry. Analytical Sciences, 2005, 21, 1031-1036.	0.8	2
226	Simultaneous Determination of Cobalt, Copper and Zinc by Energy Dispersive X-ray Fluorescence Spectrometry after Preconcentration on PAR-loaded Ion-Exchange Resin. Analytical Sciences, 2005, 21, 851-854.	0.8	50
227	Characterization of mesoporous nanocrystalline TiO2 photocatalysts synthesized via a sol-solvothermal process at a low temperature. Journal of Solid State Chemistry, 2005, 178, 321-328.	1.4	91
228	Coating MWNTs with Cu2O of different morphology by a polyol process. Journal of Solid State Chemistry, 2005, 178, 1488-1494.	1.4	53
229	Enhancement of photocatalytic activity of mesoporous TiO2 by using carbon nanotubes. Applied Catalysis A: General, 2005, 289, 186-196.	2.2	434
230	Morphology-Controllable Synthesis of Mesoporous CeO2Nano- and Microstructures. Chemistry of Materials, 2005, 17, 4514-4522.	3.2	507
231	Preparation of stable porous nickel and cobalt oxides using simple inorganic precursor, instead of alkoxides, by a sonochemical technique. Ultrasonics Sonochemistry, 2005, 12, 205-212.	3.8	36
232	Enhancement of adsorption and photocatalytic activity of TiO2 by using carbon nanotubes for the treatment of azo dye. Applied Catalysis B: Environmental, 2005, 61, 1-11.	10.8	377
233	Essential oil composition of the needles ofAbies nephrolepis Maxim from China. Flavour and Fragrance Journal, 2005, 20, 534-536.	1.2	6
234	Three-Dimensionally Ordered Mesoporous Molecular-Sieve Films as Solid Superacid Photocatalysts. Advanced Materials, 2005, 17, 99-102.	11.1	73

#	Article	lF	CITATIONS
235	Self-Assembly of ZnO Nanorods and Nanosheets into Hollow Microhemispheres and Microspheres. Advanced Materials, 2005, 17, 756-760.	11.1	396
236	A Mesoporous Pt/TiO2 Nanoarchitecture with Catalytic and Photocatalytic Functions. Chemistry - A European Journal, 2005, 11, 2997-3004.	1.7	150
237	Sonication assisted deposition of Cu2O nanoparticles on multiwall carbon nanotubes with polyol process. Carbon, 2005, 43, 670-673.	5.4	58
238	A General inâ€situ Hydrothermal Rolling-Up Formation of One-Dimensional, Single-Crystalline Lead Telluride Nanostructures. Small, 2005, 1, 349-354.	5.2	75
239	A robust three-dimensional mesoporous Ag/TiO2 nanohybrid film. Chemical Communications, 2005, , 2262.	2.2	64
240	Meso- and macro-porous Pd/CexZr1–xO2 as novel oxidation catalysts. Journal of Materials Chemistry, 2005, 15, 2193.	6.7	40
241	A Low-Temperature and Mild Solvothermal Route to the Synthesis of Wurtzite-Type ZnS With Single-Crystalline Nanoplate-like Morphology. Crystal Growth and Design, 2005, 5, 1761-1765.	1.4	68
242	Selected-Control Synthesis of NaV6O15and Na2V6O16·3H2O Single-Crystalline Nanowires. Crystal Growth and Design, 2005, 5, 969-974.	1.4	67
243	Efficient Visible-Light-Induced Photocatalytic Disinfection on Sulfur-Doped Nanocrystalline Titania. Environmental Science & Technology, 2005, 39, 1175-1179.	4.6	754
244	Photoreaction of aromatic compounds at α-FeOOH/H2O interface in the presence of H2O2: evidence for organic-goethite surface complex formation. Water Research, 2005, 39, 119-128.	5.3	63
245	Photocatalytic TiO2/Glass Nanoflake Array Films. Langmuir, 2005, 21, 3486-3492.	1.6	41
246	Fabrication of hierarchical porous iron oxide films utilizing the Kirkendall effect. Chemical Communications, 2005, , 2683.	2.2	42
247	A simple approach to reactivate silver-coated titanium dioxide photocatalyst. Catalysis Communications, 2005, 6, 684-687.	1.6	48
248	Microwave-assisted synthesis and in-situ self-assembly of coaxial Ag/C nanocables. Chemical Communications, 2005, , 2704.	2.2	50
249	Photocatalytic Activity of a Hierarchically Macro/Mesoporous Titania. Langmuir, 2005, 21, 2552-2559.	1.6	443
250	Biomimetic Synthesis of CaCO ₃ Particles with Specific Size and Morphology. Key Engineering Materials, 2005, 280-283, 601-604.	0.4	2
251	Preparation and Photocatalytic Behavior of MoS2 and WS2 Nanocluster Sensitized TiO2. Langmuir, 2004, 20, 5865-5869.	1.6	519
252	Synthesis and Characterization of Porous Magnesium Hydroxide and Oxide Nanoplates. Journal of Physical Chemistry B, 2004, 108, 64-70.	1.2	303

#	Article	IF	CITATIONS
253	Peanut-shaped nanoribbon bundle superstructures of malachite and copper oxide. Journal of Crystal Growth, 2004, 266, 545-551.	0.7	53
254	One-dimensional shape-controlled preparation of porous Cu2O nano-whiskers by using CTAB as a template. Journal of Solid State Chemistry, 2004, 177, 4640-4647.	1.4	109
255	Sono- and Photochemical Routes for the Formation of Highly Dispersed Gold Nanoclusters in Mesoporous Titania Films. Advanced Functional Materials, 2004, 14, 1178-1183.	7.8	83
256	Nonaggregated Zinc Phthalocyanine in Mesoporous Nanocrystalline TiO2 Thin Films. Macromolecular Rapid Communications, 2004, 25, 1414-1418.	2.0	12
257	A Self-Seeded, Surfactant-Directed Hydrothermal Growth of Single Crystalline Lithium Manganese Oxide Nanobelts from the Commercial Bulky Particles ChemInform, 2004, 35, no.	0.1	Ο
258	Systematic Synthesis and Characterization of Single-Crystal Lanthanide Orthophosphate Nanowires ChemInform, 2004, 35, no.	0.1	1
259	Pore-Wall Chemistry and Photocatalytic Activity of Mesoporous Titania Molecular Sieve Films ChemInform, 2004, 35, no.	0.1	0
260	Sonochemical Synthesis of Aragonite-Type Calcium Carbonate with Different Morphologies ChemInform, 2004, 35, no.	0.1	0
261	Preparation of a highly active nanocrystalline TiO2 photocatalyst from titanium oxo cluster precursor. Journal of Solid State Chemistry, 2004, 177, 2584-2590.	1.4	50
262	Selective self-propagating combustion synthesis of hexagonal and orthorhombic nanocrystalline yttrium iron oxide. Journal of Solid State Chemistry, 2004, 177, 3666-3674.	1.4	123
263	A Simple and General Method for the Synthesis of Multicomponent Na2V6O16·3H2O Single-Crystal Nanobelts. Journal of the American Chemical Society, 2004, 126, 3422-3423.	6.6	158
264	Efficient H2O2Oxidation of Organic Pollutants Catalyzed by Supported Iron Sulfophenylporphyrin under Visible Light Irradiation. Journal of Physical Chemistry B, 2004, 108, 7263-7270.	1.2	84
265	Preparation of a highly active nanocrystalline TiO2 photocatalyst from titanium oxo cluster precursor. Journal of Solid State Chemistry, 2004, 177, 2584-2584.	1.4	2
266	Pore-Wall Chemistry and Photocatalytic Activity of Mesoporous Titania Molecular Sieve Films. Chemistry of Materials, 2004, 16, 1523-1530.	3.2	254
267	Sonochemical synthesis of aragonite-type calcium carbonate with different morphologies. New Journal of Chemistry, 2004, 28, 1027.	1.4	126
268	Facile fabrication and characterization of hierarchically porous calcium carbonate microspheres. Chemical Communications, 2004, , 2414.	2.2	60
269	A General Solution-Phase Approach to Oriented Nanostructured Films of Metal Chalcogenides on Metal Foils:  The Case of Nickel Sulfide. Journal of the American Chemical Society, 2004, 126, 8116-8117.	6.6	104
270	Hydrothermal Synthesis of a Novel Sodium Vanadium Bronze with Single-crystalline Nanobelt-like Morphology. Chemistry Letters, 2004, 33, 1612-1613.	0.7	2

#	Article	IF	CITATIONS
271	Preparation and photocatalytic behavior of MoS2 and WS2 nanocluster sensitized TiO2. Langmuir, 2004, 20, 5865-9.	1.6	54
272	Preparation and characterization of highly photoactive nanocrystalline TiO2 powders by solvent evaporation-induced crystallization method. Science in China Series B: Chemistry, 2003, 46, 549.	0.8	16
273	Systematic Synthesis and Characterization of Single-Crystal Lanthanide Orthophosphate Nanowires. Journal of the American Chemical Society, 2003, 125, 16025-16034.	6.6	443
274	Photocatalytic Activity, Antibacterial Effect, and Photoinduced Hydrophilicity of TiO2Films Coated on a Stainless Steel Substrate. Environmental Science & amp; Technology, 2003, 37, 2296-2301.	4.6	359
275	Preconcentration using diethylenetriaminetetraacetic acid-functionalized polysiloxane (DETAP) for determination of molybdenum(VI) in seawater by ICP?OES. Analytical and Bioanalytical Chemistry, 2003, 376, 728-734.	1.9	21
276	Photocatalytic degradation of cationic blue X-GRL adsorbed on TiO2/SiO2 photocatalyst. Applied Catalysis B: Environmental, 2003, 40, 131-140.	10.8	103
277	Photocatalytic degradation of triazine-containing azo dyes in aqueous TiO2 suspensions. Applied Catalysis B: Environmental, 2003, 42, 47-55.	10.8	159
278	Effects of acidity and inorganic ions on the photocatalytic degradation of different azo dyes. Applied Catalysis B: Environmental, 2003, 46, 35-47.	10.8	207
279	Characterization of chemical species in PM2.5 and PM10 aerosols in Hong Kong. Atmospheric Environment, 2003, 37, 31-39.	1.9	311
280	Effects of acidic and basic hydrolysis catalysts on the photocatalytic activity and microstructures of bimodal mesoporous titania. Journal of Catalysis, 2003, 217, 69-69.	3.1	518
281	Hydrothermal Synthesis of Rare Earth (Tb, Y) Hydroxide and Oxide Nanotubes. Advanced Functional Materials, 2003, 13, 955-960.	7.8	182
282	Title is missing!. Angewandte Chemie, 2003, 115, 1059-1062.	1.6	30
283	Microemulsion-Mediated Solvothermal Synthesis of Nanosized CdS-Sensitized TiO2 Crystalline Photocatalyst ChemInform, 2003, 34, no.	0.1	0
284	Efficient Degradation of Organic Pollutants by Using Dioxygen Activated by Resin-Exchanged Iron(II) Bipyridine under Visible Irradiation. Angewandte Chemie - International Edition, 2003, 42, 1029-1032.	7.2	132
285	Direct sonochemical preparation of high-surface-area nanoporous ceria and ceria–zirconia solid solutions. Journal of Colloid and Interface Science, 2003, 260, 240-243.	5.0	122
286	Influence of solvation interactions on the zeta potential of titania powders. Journal of Colloid and Interface Science, 2003, 262, 97-100.	5.0	16
287	β-Cyclodextrin epichlorohydrin copolymer as a solid-phase extraction adsorbent for aromatic compounds in water samples. Analytica Chimica Acta, 2003, 477, 93-101.	2.6	90
288	The effect of Fâ^'-doping and temperature on the structural and textural evolution of mesoporous TiO2 powders. Journal of Solid State Chemistry, 2003, 174, 372-380.	1.4	127

#	Article	IF	CITATIONS
289	Visible light-assisted bactericidal effect of metalphthalocyanine-sensitized titanium dioxide films. Journal of Photochemistry and Photobiology A: Chemistry, 2003, 156, 235-241.	2.0	53
290	Photocatalyst TiO2 supported on glass fiber for indoor air purification: effect of NO on the photodegradation of CO and NO2. Journal of Photochemistry and Photobiology A: Chemistry, 2003, 156, 171-177.	2.0	119
291	The sonochemical preparation of a mesoporous NiO/yttria stabilized zirconia composite. Microporous and Mesoporous Materials, 2003, 60, 91-97.	2.2	15
292	Effects of alcohol content and calcination temperature on the textural properties of bimodally mesoporous titania. Applied Catalysis A: General, 2003, 255, 309-320.	2.2	117
293	Ambient Light Reduction Strategy to Synthesize Silver Nanoparticles and Silver-Coated TiO2with Enhanced Photocatalytic and Bactericidal Activities. Langmuir, 2003, 19, 10372-10380.	1.6	271
294	The Effect of Calcination Temperature on the Surface Microstructure and Photocatalytic Activity of TiO2 Thin Films Prepared by Liquid Phase Deposition. Journal of Physical Chemistry B, 2003, 107, 13871-13879.	1.2	1,113
295	Sonochemical Preparation of Nanoporous Composites of Titanium Oxide and Size-Tunable Strontium Titanate Crystals. Langmuir, 2003, 19, 7673-7675.	1.6	55
296	Effects of Trifluoroacetic Acid Modification on the Surface Microstructures and Photocatalytic Activity of Mesoporous TiO2Thin Films. Langmuir, 2003, 19, 3889-3896.	1.6	160
297	Mesoporous Structures from Supramolecular Assembly of in situ Generated ZnS Nanoparticles. Langmuir, 2003, 19, 5904-5911.	1.6	71
298	A Novel β-CDâ^'Hemin Complex Photocatalyst for Efficient Degradation of Organic Pollutants at Neutral pHs under Visible Irradiation. Journal of Physical Chemistry B, 2003, 107, 9409-9414.	1.2	65
299	Synthesis and Characterization of Phosphated Mesoporous Titanium Dioxide with High Photocatalytic Activity. Chemistry of Materials, 2003, 15, 2280-2286.	3.2	701
300	Microemulsion-mediated solvothermal synthesis of nanosized CdS-sensitized TiO2 crystalline photocatalystElectronic supplementary information (ESI) available: UV-visible absorption spectra, XRD patterns and EPR spectrum. See http://www.rsc.org/suppdata/cc/b3/b302418k/. Chemical Communications, 2003, , 1552.	2.2	118
301	Efficient degradation of organic pollutants mediated by immobilized iron tetrasulfophthalocyanine under visible light irradiation. Chemical Communications, 2003, , 80-81.	2.2	33
302	A highly selective photooxidation approach using O2 in water catalyzed by iron(ii) bipyridine complex supported on NaY zeolite. Chemical Communications, 2003, , 2214.	2.2	27
303	A sonochemical approach to hierarchical porous titania spheres with enhanced photocatalytic activityElectronic Supplementary Information (ESI) available: XRD patterns, nitrogen adsorption/desorption isotherms, pore size distribution curves, photocatalytic activities and physicochemical properties of HPT and SMT. See http://www.rsc.org/suppdata/cc/b3/b306013f/. Chemical A self-seeded, surfactant-directed hydrothermal growth of single crystalline lithium manganese	2.2	212
304	oxide nanobelts from the commercial bulky particlesElectronic supplementary information (ESI) available: SEM images of commercial lithium manganese oxide bulky particles and the products synthesized under different conditions as well as lithium manganese oxide nanobelts, Se nanorods and MnO2 nanorods grown on the bulky particles and Te nanotubes. See	2.2	48
305	http://www.rsc.org/suppdata/cc/b3/b310998d/. Chemical Communications, 2003, , 2910. The sonochemical preparation of lamellar MoOx. Journal of Materials Chemistry, 2003, 13, 2851.	6.7	4
306	Determination of Manganese (II) in Foodstuffs by β-Cyclodextrin Polymer Phase Spectrophotometry with 1-(2-Pyridylazo)-2-naphthol. Supramolecular Chemistry, 2002, 14, 373-378.	1.5	2

#	Article	IF	CITATIONS
307	DETERMINATION OF COBALT IN FOODS BY Î ² -CYCLODEXTRIN POLYMER PHASE SPECTROPHOTOMETRY USING 2-(5-BROMO-2-PYRIDYLAZO)-5-DIETHYLAMINOPHENOL. Analytical Letters, 2002, 35, 825-835.	1.0	2
308	Continuous Formation of Supported Unusual Mesostructured Silica Films by Solâ^'Gel Dip Coating. Langmuir, 2002, 18, 9570-9573.	1.6	18
309	Effects of calcination temperature on the photocatalytic activity and photo-induced super-hydrophilicity of mesoporous TiO2 thin films. New Journal of Chemistry, 2002, 26, 607-613.	1.4	247
310	The preparation of a highly ordered long-range lamellar silica structure with large interlayer spacingsElectronic supplementary information (ESI) available: Figs. S1–3: XRD, adsorption–desorption isotherms and SEM image. See http://www.rsc.org/suppdata/cc/b2/b204053k/. Chemical Communications, 2002, , 1614-1615.	2.2	19
311	Effect of surface microstructure on the photoinduced hydrophilicity of porous TiO2 thin films. Journal of Materials Chemistry, 2002, 12, 81-85.	6.7	89
312	Photo-Fenton degradation of malachite green catalyzed by aromatic compounds under visible light irradiation. New Journal of Chemistry, 2002, 26, 336-341.	1.4	67
313	Degradation of azo dye Procion Red MX-5B by photocatalytic oxidation. Chemosphere, 2002, 46, 905-912.	4.2	305
314	Determination of total gaseous selenium in atmosphere by honeycomb denuder/differential pulse cathodic stripping voltammetry. Talanta, 2002, 57, 323-331.	2.9	23
315	Direct Sonochemical Preparation and Characterization of Highly Active Mesoporous TiO2 with a Bicrystalline Framework. Chemistry of Materials, 2002, 14, 4647-4653.	3.2	325
316	Rapid synthesis of mesoporous TiO2 with high photocatalytic activity by ultrasound-induced agglomeration. New Journal of Chemistry, 2002, 26, 416-420.	1.4	136
317	Carbonaceous characteristics of atmospheric particulate matter in Hong Kong. Science of the Total Environment, 2002, 300, 59-67.	3.9	69
318	Enhanced photocatalytic activity of mesoporous and ordinary TiO2 thin films by sulfuric acid treatment. Applied Catalysis B: Environmental, 2002, 36, 31-43.	10.8	450
319	Photooxidation of azo dye in aqueous dispersions of H2O2/α-FeOOH. Applied Catalysis B: Environmental, 2002, 39, 211-220.	10.8	157
320	Hierarchically Ordered Silica Mesophases Using Mixed Surfactant Systems as Templates. Angewandte Chemie - International Edition, 2002, 41, 3844-3848.	7.2	21
321	Oxide Monoliths and Films with Unusual Long-Range Highly Ordered Lamellar Structures. Advanced Materials, 2002, 14, 1064.	11.1	28
322	Enhancing effects of water content and ultrasonic irradiation on the photocatalytic activity of nano-sized TiO2 powders. Journal of Photochemistry and Photobiology A: Chemistry, 2002, 148, 263-271.	2.0	173
323	Light-induced super-hydrophilicity and photocatalytic activity of mesoporous TiO2 thin films. Journal of Photochemistry and Photobiology A: Chemistry, 2002, 148, 331-339.	2.0	131
324	Bactericidal and photocatalytic activities of TiO2 thin films prepared by sol–gel and reverse micelle methods. Journal of Photochemistry and Photobiology A: Chemistry, 2002, 153, 211-219.	2.0	51

#	Article	IF	CITATIONS
325	Simultaneous determination of inorganic anions, carboxylic and aromatic carboxylic acids by capillary zone electrophoresis with direct UV detection. Journal of Chromatography A, 2002, 942, 289-294.	1.8	26
326	Effects of F-Doping on the Photocatalytic Activity and Microstructures of Nanocrystalline TiO2Powders. Chemistry of Materials, 2002, 14, 3808-3816.	3.2	2,068
327	Photocatalytic Activity and Characterization of the Sol-Gel Derived Pb-Doped TiO2 Thin Films. Journal of Sol-Gel Science and Technology, 2002, 24, 39-48.	1.1	80
328	The Effect of SiO2 Addition on the Grain Size and Photocatalytic Activity of TiO2 Thin Films. Journal of Sol-Gel Science and Technology, 2002, 24, 95-103.	1.1	81
329	Atomic Force Microscopic Studies of Porous TiO2 Thin Films Prepared by the Sol-Gel Method. Journal of Sol-Gel Science and Technology, 2002, 24, 229-240.	1.1	29
330	ION CHROMATOGRAPHIC SEPARATION OF ANIONS AND CATIONS ON A TITANIA PACKED COLUMN. Journal of Liquid Chromatography and Related Technologies, 2001, 24, 367-380.	0.5	12
331	Preparation of highly photocatalytic active nano-sized TiO2 particles via ultrasonic irradiation. Chemical Communications, 2001, , 1942-1943.	2.2	321
332	Determination of lead in fine particulates by slurry sampling electrothermal atomic absorption spectrometry. Fresenius' Journal of Analytical Chemistry, 2001, 369, 170-175.	1.5	8
333	Separation and determination of Cr(III) by titanium dioxide-filled column and inductively coupled plasma mass spectrometry. Analytica Chimica Acta, 2001, 436, 59-67.	2.6	30
334	Title is missing!. Journal of Materials Science Letters, 2001, 20, 1745-1748.	0.5	89
335	Separation and Detection of Metal Ions in Ecological Samples by Capillary Zone Electrophoresis with Indirect UV Detection. Journal of High Resolution Chromatography, 2000, 23, 511-514.	2.0	10
336	Polymeric membrane silver-ion selective electrodes based on bis(dialkyldithiophosphates). Analytica Chimica Acta, 2000, 416, 139-144.	2.6	39
337	Direct determination of mercury in atmospheric particulate matter by graphite plate filtration–electrothermal atomic absorption spectrometry with Zeeman background correction. Spectrochimica Acta, Part B: Atomic Spectroscopy, 2000, 55, 395-402.	1.5	4
338	Influence of Thermal Treatment on the Adsorption of Oxygen and Photocatalytic Activity of TiO2. Langmuir, 2000, 16, 7304-7308.	1.6	112
339	VIRTUAL CLASSROOM AS A TOOL FOR ENVIRONMENTAL EDUCATION. , 2000, , .		0
340	Photocatalytic Activity of Rutile Ti1â^'xSnxO2Solid Solutions. Journal of Catalysis, 1999, 183, 368-372.	3.1	287
341	Simultaneous Determination of Inorganic Anions and Organic Acids in Environmental Samples by Capillary Zone Electrophoresis with Indirect UV Detection. Journal of High Resolution Chromatography, 1999, 22, 379-385.	2.0	22
342	Speciation and distribution of trihalomethanes in the drinking water of Hong Kong. Environment International, 1999, 25, 605-611.	4.8	9

#	Article	IF	CITATIONS
343	Potentiometric detection of ascorbate using a graphite carbon electrode. Talanta, 1999, 49, 661-665.	2.9	7
344	Simultaneous determination of Co(II), Cr(VI), Ni(II) and Pb(II) in water by solvent extraction and high-field 1 H NMR Spectrometry. Fresenius' Journal of Analytical Chemistry, 1998, 361, 210-213.	1.5	1
345	An investigation on photocatalytic activities of mixed TiO2-rare earth oxides for the oxidation of acetone in air. Journal of Photochemistry and Photobiology A: Chemistry, 1998, 116, 63-67.	2.0	261
346	Electromagnetic Induction in Inductively Coupled Plasma. Journal of Chemical Education, 1998, 75, 316.	1.1	0
347	Ti1-xZrxO2Solid Solutions for the Photocatalytic Degradation of Acetone in Air. Journal of Physical Chemistry B, 1998, 102, 5094-5098.	1.2	205
348	Photocatalytic Degradation of a Gaseous Organic Pollutant. Journal of Chemical Education, 1998, 75, 750.	1.1	16
349	Enhanced photocatalytic activity of Ti1â^'xVxO2 solid solution on the degradation of acetone. Journal of Photochemistry and Photobiology A: Chemistry, 1997, 111, 199-203.	2.0	83
350	Flow injection solid-phase chemiluminescent immunoassay using a membrane-based reactor. Analytical Chemistry, 1991, 63, 666-669.	3.2	44
351	Semiconductor olefin adducts. Photoluminescent properties of cadmium sulfide and cadmium selfide and cadmium selenide in the presence of butenes. Journal of the American Chemical Society, 1989, 111, 5146-5148.	6.6	33
352	Dithiocarbamate extraction of gallium from natural waters and from biological samples for neutron activation analysis. Analytical Chemistry, 1984, 56, 1689-1691.	3.2	50
353	Extraction of gold and mercury from sea water with bismuth diethyldithiocarbamate prior to neutron activation—γ-spectrometry. Analytica Chimica Acta, 1983, 154, 307-312.	2.6	63
354	Solvent extraction of dithiocarbamate complexes and back-extraction with mercury(II) for determination of trace metals in seawater by atomic absorption spectrometry. Analytical Chemistry, 1982, 54, 2536-2539.	3.2	106
355	Photocatalysts for Solar-Induced Water Disinfection: New Developments and Opportunities. Materials Science Forum, 0, 734, 63-89.	0.3	13